Published in final edited form as:
J Biomech. 2011 June 3; 44(9): 1729–1734. doi:10.1016/j.jbiomech.2011.03.037.

Optical Measurements of Vocal Fold Tensile Properties: Implications for Phonatory Mechanics

Jordan E. Kelleher[1], **Thomas Siegmund**[1,*], **Roger W. Chan**[2], and **Erin A. Henslee**[2]

[1]Mechanical Engineering, Purdue University, West Lafayette, IN

[2]Otolaryngology–Head and Neck Surgery; and Biomedical Engineering, University of Texas Southwestern Medical Center, Dallas, TX

Abstract

In voice research, *in vitro* tensile stretch experiments of vocal fold tissues are commonly employed to determine the tissue biomechanical properties. In the standard stretch-release protocol, tissue deformation is computed from displacements applied to sutures inserted through the thyroid and arytenoid cartilages, with the cartilages assumed to be rigid. Here, a non-contact optical method was employed to determine the actual tissue deformation of vocal fold lamina propria specimens from three excised human larynges in uniaxial tensile tests. Specimen deformation was found to consist not only of deformation of the tissue itself, but also deformation of the cartilages, as well as suture alignment and tightening. Stress-stretch curves of a representative load cycle were characterized by an incompressible Ogden model. The initial longitudinal elastic modulus was found to be considerably higher if determined based on optical displacement measurements than typical values reported in the literature. The present findings could change the understanding of the mechanics underlying vocal fold vibration. Given the high longitudinal elastic modulus the lamina propria appeared to demonstrate a substantial level of anisotropy. Consequently, transverse shear could play a significant role in vocal fold vibration, and fundamental frequencies of phonation should be predicted by beam theories accounting for such effects.

Keywords

Vocal folds; Elasticity; Biomechanical testing; Optical measurements; Fundamental frequency

1. Introduction

The importance of image-based deformation measurements of soft tissues in order to avoid local stress concentrations and local deformations has long been recognized (Yin et al., 1972; Lanir and Fung, 1974). Protocols in the cardiac biomechanics field routinely employ optical deformation measurements (Fronek et al., 1976). However, such an approach has not yet been applied in the characterization of vocal fold tissues. In our recent work, the digital

*Corresponding author siegmund@purdue.edu, phone: (765) 494 9766; Fax: (765) 494-0539; Mail: 585 Purdue Mall, West Lafayette, IN 47907, U.S.A..

Conflict of interest statement None declared.

image correlation method was applied to characterize tissue deformation at one time point in a tensile stretch-relaxation experiment (Kelleher et al., 2010). This study indicated that the applied tensile deformation was significantly larger than the deformation of the tissue itself. How such discrepancies might affect the mechanical characteristics of the tissue under a sequence of stretch cycles remains unknown. Therefore, we hypothesized that the true deformation of a vocal fold tissue specimen would differ from the deformation applied by the stretch-release apparatus; hence, the tissue biomechanical properties would be different from what has been reported in the past.

Biomechanical experiments of vocal fold tissues began by simply hanging weights on specimens and measuring the displacements visually (Kakita et al., 1981). This technique was unable to produce a stress-stretch curve accounting for nonlinearity and only order-of-magnitude estimations of the elastic modulus were obtained. A more precise *in vitro* experimental apparatus was developed using servo-motors to apply displacements to specimens held in a physiological solution (Perlman and Titze, 1988). Throughout the past 20 years, this method has been followed by many studies on various laryngeal tissues (Perlman et al., 1984; Alipour-Haghighi and Titze, 1985, 1987, 1991, 1999; Perlman and Titze, 1988; Perlman and Alipour-Haghighi, 1988; Alipour-Haghighi et al., 1989, 2010; Min et al., 1995; Zhang et al., 2006, 2007, 2009; Chan et al., 2007; Hunter and Titze, 2007; Riede et al., 2010).

In vivo indentation-type loading was applied by (Berke and Smith, 1992; Tran et al., 1993). A force gauge was brought into slight contact with the vocal fold; the recurrent laryngeal nerve was stimulated with electric current causing vocal fold adduction and deflecting the gauge. From force-deflection data and known areas of contact, the elastic modulus was estimated. In a laryngeal tensiometer (Hess et al., 2006) a probe is attached to the vocal fold via a pin, suction, or adhesion, applying a shear or an indentation force from which the elastic spring rate and a shear modulus were determined (Goodyer et al., 2006, 2007). However, complications exist with the quantitative determination of biomechanical properties as calculations of moduli based on average bearing stresses are unreliable and adhesion of the probe is difficult to ensure on the moist tissue surfaces. Also, such device do not distinguish between the various layers of the vocal fold - an important aspect for phonosurgeons and tissue engineers creating biomaterials and implants for vocal fold reconstruction (Kutty and Webb, 2009). *In vivo* non-contact methods based on ultrasound (Hsiao et al., 2002), air pulse stimulation (Hertegård et al., 2009), and high speed video (HSV) techniques (Döllinger et al., 2002; Tao et al., 2007; Qin et al., 2009) have been proposed. The ultrasound method must assume a model (e.g. string or beam model) *a priori*, and allows for the calculation of moduli based upon measured deformation and the frequency of vibration. For HSV techniques the compact nature of these models is often overshadowed by their need for numerous biomechanical tissue parameters in the lumped mass models underpinning the method. HSV studies (e.g., Döllinger et al., 2002; Tao et al., 2007; Qin et al., 2009) and some experimental studies of laryngeal tissues (Goodyer et al., 2006, 2007) have reported values in terms of stiffness (force/length and structural damping) rather than standard mechanics terminology such as elastic moduli. Such characteristics are difficult to compare to other true moduli.

2. Materials and Methods

2.1 Experiments

Tissue specimens isolated from the excised larynges of three male human cadaveric subjects were considered, Table 1. For each subject, one vocal ligament specimen and the contralateral vocal fold cover specimen were tested.[1] Following the protocol of Chan et al. (2007), the cover and ligament specimens were dissected with instruments for

phonomicrosurgery, separated from the underlying muscle and immediately placed in phosphate buffered saline (PBS). Figure 1 shows schematic drawings of the relevant anatomical structures.

3-0 nylon sutures[2] were inserted through the center of the arytenoid cartilage and the center of the thyroid cartilage both naturally attached to the vocal ligament or cover specimens. The suture inserted through the thyroid cartilage section was connected to the actuator (lever arm) of a servo-controlled lever system,[3] while the suture inserted through the arytenoid cartilage section was connected to the support. Figure 2 depicts the experimental setup. The lever system was under displacement feedback control, and was connected to a function generator and an oscilloscope to monitor the displacement input. The tensile force response of the specimen was detected by the lever system, digitized at 500 samples/s and output for further analysis. The applied displacement was sinusoidal at 1 Hz with an amplitude of 3–5 mm, depending upon the initial, resting vocal fold length L_0. The tensile test was conducted for 300 cycles.

A monochrome CCD camera[4] (pixel size of 9.9 × 9.9 μm, maximum frame rate of 75 fps) together with a macro lens[5] was used to capture images continuously during the experiment. A level was used to ensure that the optical path of the camera was perpendicular to the specimen axis. A traceable speckle pattern was applied by applying (1) a spray-on cosmetic foundation sparingly to the moist tissue, and (2) black ink dots with a fine tipped paint brush onto the cosmetic foundation. The foundation inhibited fading of the ink on the moist tissue. This procedure resulted in a covering of the tissue with a discontinuous speckle pattern such that specimen stiffness and moisture ingress were not disturbed. During the experiments, specimens were kept in air to avoid optical distortions related to a glass chamber with physiological solution as well as dissolution of the ink. Instead, specimens were hydrated periodically by dripping PBS onto the thyroid cartilage. Displacements of points on the specimen surface were obtained from image sequences via digital image correlation functions of the Image Processing Toolbox™ of MATLAB® (The MathWorks, Inc., Natick, MA). Distance measurements were calibrated by taking an image of an object of known dimensions to establish a pixel-to-mm ratio. Details of the software script are provided in the online supplemental material.

2.2 Analytical

The nominal stress in the tissue, $\sigma=F/A_0$, was determined from the force output from the load cell F and the average cross-section area A_0 in the undeformed state. The tissue specimen was assumed to have circular cross-sections. A second CCD camera, offset by approximately 30° to the first, confirmed the circular cross-sections to be a reasonable assumption. The cross-sectional diameter D_0 was determined from specimen images as the average of ten diameter measurements at equidistant axial locations. The initial, undeformed length L_0 of the tissue specimen, defined as the vocal fold mounting length from the vocal process to the anterior commissure, was measured with digital calipers once the specimen was positioned in the experimental apparatus, Table 1. Under the standard assumption of rigid cartilages (arytenoid and thyroid), the elongation e of the tissue is assumed to be equal to the displacement applied by the lever arm, $e = u_L$. Then, the stretch of the tissue specimen based on the lever arm λ_L is

[1]The sample preparation and testing protocols were approved by the Institutional Review Board of UT Southwestern Medical Center, Dallas, Texas, USA.
[2]ETHILON* Nylon Suture, © Ethicon, Inc.
[3]Aurora Scientific Model 300B-LR, Aurora, Ontario, Canada.
[4]Allied Vision Technologies, Stingray F-033B.
[5]Tamron SP 90 mm F/2.8 Macro, Tamron Co., Ltd., Saitama, Japan.

$$\lambda_L = 1 + \frac{\mu_L}{L_0}. \quad (1)$$

The elongation of the tissue specimen was also determined from the optically measured displacements, u_1, u_2, of two points – one located at the vocal process and one at the anterior commissure – as $e = u_1 - u_2$. The stretch based on imaging λ_I is then

$$\lambda_I = 1 + \frac{\mu_1 - \mu_2}{L_0}. \quad (2)$$

The deformation of vocal fold tissues can be characterized well by a hyperelastic, large strain constitutive model (Zhang et al., 2006, 2007). In a first-order, incompressible Ogden model (Ogden, 1972) the stress-stretch relationship under uniaxial loading is

$$\sigma = \frac{2E}{3\alpha}\left[\lambda^{\alpha-1} - \lambda^{-\left(1+\frac{1}{2}\alpha\right)}\right] \quad (3)$$

with E being the initial longitudinal elastic modulus, α a real number characteristic of the nonlinearity of the tissue response, and λ either λ_L or λ_I depending on the approach. The stress-stretch equilibrium response, estimated as the midpoint values of the loading and unloading portions of the hysteresis loop was fitted to Eq. (3) by the Levenberg-Marquardt nonlinear least-squares optimization algorithm (Levenberg, 1944; Marquardt, 1963).

3. Results

All vocal fold tissue specimens exhibited a time dependent response with the stress at maximum applied stretch declining continuously with the number of applied load cycles, consistent with previous observations (Zhang et al., 2009). No “stabilized state” was apparently reached. From cycles N =1 to N = 300, the average peak stress decayed by 20% (see Table A1 in the online supplemental material). The detailed analysis of the tissue specimens was conducted for cycle N = 55 where the peak stress had experienced on average 63% of the total decay. The 55th cycle was also chosen because it provided a high image frame rate for all specimens.

The reasons for the differences between λ_I and λ_L are apparent in Figure 3. Both the thyroid and arytenoid cartilages were found to deform considerably. On average, the collective elongation of the cartilages (thyroid and arytenoid) contributed approximately 30% of the total applied displacement (Table 2). Clearly, the cartilages should not be considered as rigid bodies. Furthermore, suture alignment and tightening of the suture loop along with some amount of specimen rotation was observed (characterized as u_{other} in Table 2). These processes take up between 34% and 57% of the applied displacement. However, the elongation of the sutures themselves in the suture loop (e_s) is negligible as $e_s = (1/2)(F_{max}L_0)/(0.25\pi D^2 E) = 0.08$ mm considering F_{max} = 0.2 N, L_0 = 50 mm, D = 0.2 mm for 3-0 sutures, and E = 2,000 MPa for nylon sutures (Holmlund, 1976; García Páez et al., 1996).

Figure 3 depicts the two specimens (ligament and cover) of subject C at λ=1 and $\lambda=\lambda_{max}$, and the corresponding stress-stretch curves are given in Figure 4. The stress-stretch curves based on displacements from the lever arm, σ-λ_L, and from the image sequences, σ-λ_I, respectively, displayed qualitatively similar shapes. However, λ_L was considerably larger than λ_I for both the cover and the ligament. The parameters of the Ogden model were

determined for fits to the σ-λ_L and σ-λ_I curves as (E_L, α_L) and (E_I, α_I), respectively (Table 3). The tissue longitudinal elastic modulus obtained from the imaging protocol, E_I, was prominently larger than that obtained from the lever arm displacement, E_L. Similarly, the degree of nonlinearity of the σ-λ curves was substantially greater when based on the imaging data, $\alpha_I > \alpha_L$. The correction factors, $C_E = E_I/E_L$ and $C_\alpha = \alpha_I/\alpha_L$, provide a quantitative comparison among the Ogden model parameters derived from the two approaches (Table 3).

4. Discussion

4.1 Experiments

Using a standard *in vitro* tensile test on human vocal fold tissues (Perlman et al., 1984; Alipour-Haghighi and Titze, 1985, 1987, 1991, 1999; Perlman and Titze, 1988; Perlman and Alipour-Haghighi, 1988; Alipour-Haghighi et al., 1989, 2010; Min et al., 1995; Zhang et al., 2006, 2007, 2009; Chan et al., 2007; Hunter and Titze, 2007; Riede et al., 2010), the longitudinal elastic modulus of the low-stretch, linear regime has been found to be around 10–30 kPa for the vocal ligament (Min et al., 1995; Chan et al., 2007) and 5–20 kPa for the vocal fold cover (Zhang et al., 2006; Chan et al., 2007). The degree of nonlinearity of the vocal fold cover ranges from 14.4–19.5 for elderly subjects (Zhang et al., 2006). The values for E_L and α_L obtained in the present study are well within the range of values reported in earlier studies. However, it was found that the lever arm data consistently overestimated the tissue deformation. Hence, the elastic moduli (E_I) and the degree of nonlinearity (α_I) derived from stretch data based on the image sequences were substantially higher. The 55^{th} cycle was chosen as a representative stretch cycle. The Ogden parameters would quantitatively vary depending upon the cycle number N due to the peak stress decay; however, the qualitative results and conclusions would remain the same.

The present values for C_E and C_α are preliminary and should be used with caution. These correction factors may be dependent on a number of variables that are not yet well defined and understood, such as the details of the dissection process, the suturing technique, postmortem hours, and age and gender of the tissue specimens. According to the present findings, previous results may have underestimated the longitudinal elastic modulus of the vocal fold cover approximately by a factor of five and the degree of nonlinearity by a factor of three. Still, the present study was based only on a limited number of specimens. The suturing technique and mounting was also partially responsible for the differences in λ_L and λ_I. A single suture connected to the lever arm (as in Chan et al., 2007), may avoid suture slack more readily, but was found to lead to more undesired specimen rotation during testing. The looped suture arrangement employed here was observed to minimize specimen rotation. One feasible solution may be to clamp the cartilages, e.g., Riede et al. (2010) substituted the suture in the arytenoid cartilage with a clamp. The use of optical methods to measure the actual tissue deformation, however, largely eliminated the negative influence of any cartilage deformation and suturing techniques on the measurement accuracy of specimen elongation. Potential errors existing in the proposed technique are described in detail in the supplemental material online. These errors are not estimated to alter the finding of a significant difference between the lever arm based data and the optical measurements.

The percentage of the lever arm displacement that was not found in the specimen (Table 2) was large. However, the Ogden model parameters based upon stretch values calculated from the lever arm displacements are within the 95% confidence interval of those calculated in previous studies with a similar protocol (Zhang et al., 2006). Thus, one can speculate that there may have been a considerable portion of the lever arm displacement occurring outside the specimen in all previous investigations, most likely due to suture-related effects. For an in-depth analysis of the suture-related displacements, see the supplemental material online.

4.2 Analytical

If corroborated in future studies, the present findings could have significant implications for phonatory mechanics. Considering vocal fold vibration to emerge from a beam vibration-type mode of deformation, the Euler-Bernoulli beam theory predicts the fundamental frequency of vibration for a simply supported beam with circular cross-sections of diameter D_0 as

$$F_{0,EB}=\left(\frac{\pi}{L_0}\right)^2\sqrt{\frac{ED_0^2}{16\rho}} \tag{4}$$

where ρ is the density (ρ=1040 kg/m^3), and L_0 is the length of the vocal fold. However, the fundamental frequency of phonation F_0 should be considered to depend also on tissue anisotropy (i.e. either the ratio of longitudinal elastic modulus to transverse elastic modulus, or the ratio of longitudinal elastic modulus to longitudinal shear modulus) (Kelleher et al., 2010), similar to findings for engineering solids (Dudek, 1970; Larsson, 1991; Ekel'chik, 2007). Histological studies of the vocal ligament have shown a strong alignment of collagen fibers in the anterior-posterior direction (Hirano et al., 1982; Ishii et al., 1996; Gray et al., 2000; Madruga de Melo et al., 2003). Studies on the transverse shear modulus G_T of vocal fold tissues have reported values in the range of 0.1–3.5 kPa with an average around 1 kPa at phonatory frequencies (Goodyer et al., 2007; Chan and Rodriguez, 2008). As no experimental data for the longitudinal shear modulus G_L exists, micromechanical material models lead to the conclusion that for a material with perfectly aligned fibers G_L would be less than G_T (Clyne and Withers, 1993; Daniel and Ishai, 2006). Thus, if it is assumed that $G_L \approx G_T \approx 1$ kPa, a conservative estimate of the anisotropy can be obtained. Based on the average longitudinal elastic moduli obtained in this study, Table 3, anisotropy ratios (E/G_L) may be greater than 50 for both the ligament and the cover. At such high levels of anisotropy, transverse shear deformation would be pronounced and Timoshenko's beam theory is then appropriate. Solving the frequency equations in this framework is complex and in some cases they cannot be solved explicitly. If one neglects terms coupling the transverse shear and rotatory inertia an approximation can be made which is still highly accurate for frequency predictions (Egle, 1969). Then, the fundamental frequency for a simply supported beam is

$$\frac{F_0}{F_{0,EB}}=\sqrt{\frac{1+\frac{E}{kG_L}\zeta}{\left(1+\frac{E}{kG_L}\zeta\right)^2+\zeta}} \tag{5}$$

where $\zeta=(\pi D_0)^2)/(4L_0)^2$ and the transverse shear coefficient, k = 0.9643, for an incompressible beam with circular cross-sections (Hutchinson, 2001). Results based on the current average data for L_0, D_0 from Table 1 are displayed in Figure 5. For the vocal ligament and the vocal fold cover, $F_{0,EB}$ are predicted to be 234 and 254 Hz, respectively. With the present values of elastic moduli, values of $F_{0,EB}$ are much higher than the normal F_0 range of human speech, typically around 100–165 Hz for adult males (Titze, 2000). Once the anisotropy was considered (E/G_L=61 for the ligament and E/G_L=89 for the cover), F_0 significantly decreased to a more physiologically relevant range of phonation, 143 Hz and 155 Hz for the ligament and the cover, respectively. A sensitivity analysis was conducted for the model predictions. The sensitivity of predicted F_0 values to changes in E can be deduced from Figure 5. Assuming G_L as constant and changing E by ±20% results in less than 7% change to F_0. Clearly, the representation of vocal folds as simply-supported beams is a

simplification. Nevertheless, the Timoshenko beam model succinctly shows the influences of anisotropy and small length-to-thickness ratios on the fundamental frequency of phonation. An improved model should also include the thyroarytenoid muscle and its stiffening influence represented as a foundation in the beam model.

The current findings may also have implications for the design and bioengineering of functional tissue replacements for the surgical repair of vocal fold lamina propria defects, such as scarring and atrophy. Tissue engineering scaffolds and bioimplants for the vocal fold cover and the vocal ligament may need to demonstrate a considerable level of tissue anisotropy, such that the repaired vocal folds could achieve a satisfactory range of fundamental frequency during phonation. To provide better functional guidelines and design criteria, further studies are warranted to quantify the vocal fold tissue anisotropy in terms of modulus ratios, such as the longitudinal elastic modulus to longitudinal shear modulus ratio (E/G_L).

5. Conclusion

Uniaxial tensile tests were performed on the vocal fold lamina propria of three human excised larynges. A CCD camera was used to capture images of the deformation throughout the load cycles and subsequently the stretch history was recovered from analyzing the images. In future work the image based deformation measurement should be combined with the controls of the stretch-stress apparatus to also ensure appropriate control of the stretch rate. A prominent difference was found between the applied displacement and the deformation of the specimen calculated from the images. Consequently, the vocal fold lamina propria appeared to demonstrate a substantially higher elastic stiffness than previously reported, with the new data indicating the possibility that previous studies might have underestimated the elastic modulus by a factor of approximately five. With the new data on the elastic moduli, the classic Euler-Bernoulli beam theory would predict fundamental frequencies outside the range of normal human phonation. Yet it was also shown that the Timoshenko beam theory could reconcile the predicted frequency ranges with actual phonation data. This beam theory appears extremely relevant for human phonation due to the small length to thickness ratio and the potentially high degree of tissue anisotropy of the vocal folds. Such a beam model is slightly more complex but would yield much insight into the mechanics of phonation. If axial strains and transverse shear are both present simultaneously, vocal fold posturing would possess two degrees of freedom. How the control of fundamental frequency can occur in such a scenario is a subject of future research.

Supplementary Material

Refer to Web version on PubMed Central for supplementary material.

Acknowledgments

The authors are grateful to the National Institutes of Health (NIDCD Grant R01 DC006101) for funding this investigation. Jordan E. Kelleher is thankful to the National Science Foundation for support in the form of a graduate research fellowship. We would also like to thank Prof. Luc Mongeau at McGill University for suggesting the method for applying a speckle pattern.

References

Alipour-Haghighi F, Jaiswal S, Vigmostad S. Vocal fold elasticity in the pig, sheep, and cow larynges. Journal of Voice. 2010 in press.

Alipour-Haghighi F, Titze IR. Viscoelastic modeling of canine vocalis muscle in relaxation. Journal of the Acoustical Society of America. 1985; 78:1939–1943. [PubMed: 4078169]

Alipour-Haghighi F, Titze IR. Twitch response in the canine vocalis muscle. Journal of Speech and Hearing Research. 1987; 30:290–294. [PubMed: 3669635]

Alipour-Haghighi F, Titze IR. Elastic models of vocal fold tissues. Journal of the Acoustical Society of America. 1991; 90:1326–1331. [PubMed: 1939897]

Alipour F, Titze IR. Active and passive characteristics of the canine cricothyroid muscles. Journal of Voice. 1999; 13:1–10. [PubMed: 10223670]

Alipour-Haghighi F, Titze IR, Perlman AL. Tetanic contraction in vocal fold muscle. Journal of Speech and Hearing Research. 1989; 32:226–231. [PubMed: 2739373]

Berke GS, Smith ME. Intraoperative measurement of the elastic modulus of the vocal fold. Part 2. Preliminary results. Laryngoscope. 1992; 102:770–778. [PubMed: 1614248]

Chan RW, Fu M, Young L, Tirunagari N. Relative contributions of collagen and elastin to elasticity of the vocal fold under tension. Annals of Biomedical Engineering. 2007; 35:1471–1483. [PubMed: 17453348]

Chan RW, Rodriguez ML. A simple-shear rheometer for linear viscoelastic characterization of vocal fold tissues at phonatory frequencies. Journal of the Acoustical Society of America. 2008; 124:1207–1219. [PubMed: 18681608]

Clyne, TW.; Withers, PJ. An Introduction to Metal Matrix Composites. Cambridge University Press; 1993. p. 12-20.

Daniel, IM.; Ishai, O. Engineering Mechanics of Composite Materials. 2nd ed.. Oxford University Press; New York and Oxford: 2006. p. 49-57.

Döllinger M, Hoppe U, Hettlich F, Lohscheller J, Schuberth S, Eysholdt U. Vibration parameter extraction from endoscopic image series of the vocal folds. IEEE Transactions on Biomedical Engineering. 2002; 49:773–781. [PubMed: 12148815]

Dudek TJ. Young's and shear moduli of unidirectional composites by a resonant beam method. Journal of Composite Materials. 1970; 4:232–241.

Egle DM. An approximate theory for transverse shear deformation and rotatory inertia effects in vibrating beams. NASA CR-1317. 1969

Ekel'chik VS. Resonance methods for determining the complex shear moduli of orthotropic composites. Mechanics of Composite Materials. 2007; 43:487–502.

Fronek K, Schmid-Schoenbein G, Fung YC. A noncontact method for three-dimensional analysis of vascular elasticity in vivo and in vitro. Journal of Applied Physiology. 1976; 40:634–637. [PubMed: 931885]

García Páez JM, Carrera San Martin A, Garcia Sestafe JV, Jorge-Herrero E, Navidad R, Cordón A, Candela I, Castillo-Olivares JL. Comparison of elasticities of components of a cardiac bioprothesis leaflet. Journal of Biomedical Materials Research. 1996; 30:47–52. [PubMed: 8788105]

Goodyer E, Hemmerich S, Müller F, Kobler J, Hess M. The shear modulus of the human vocal fold, preliminary results from 20 larynxes. European Archives of Oto-Rhino-Laryngology. 2007; 264:45–50. [PubMed: 16924433]

Goodyer E, Müller F, Bramer B, Chauhan D, Hess M. In vivo measurement of the elastic properties of the human vocal fold. European Archives of Oto-Rhino-Laryngology. 2006; 263:455–462. [PubMed: 16496110]

Gray SD, Titze IR, Alipour F, Hammond TH. Biomechanical and histological observations of vocal fold fibrous proteins. Annals of Otology, Rhinology and Laryngology. 2000; 109:77–85.

Hertegård S, Larsson H, Nagubothu SSR, Tolf A, Svensson B. Elasticity measurements in scarred rabbit vocal folds using air pulse stimulation. Logopedics Phoniatrics Vocology. 2009; 34:190–195.

Hess M, Müller F, Kobler J, Zeitels SM, Goodyer EN. Measurements of vocal fold elasticity using the linear skin rheometer. Folia Phoniatrica et Logopaedica. 2006; 58:207–216. [PubMed: 16636568]

Hirano M, Kakita Y, Ohmaru K, Kurita S. Structure and mechanical properties of the vocal fold. Speech Language. 1982; 7:271–297.

Holmlund DEW. Physical properties of surgical suture materials. Annals of Surgery. 1976; 184:189–193. [PubMed: 952566]

Hsiao TY, Wang CL, Chen CN, Hsieh FJ, Shau YW. Elasticity of human vocal folds measured *in vivo* using color Doppler imaging. Ultrasound in Medicine & Biology. 2002; 28:1145–1152. [PubMed: 12401384]

Hunter EJ, Titze IR. Refinements in modeling the passive properties of laryngeal soft tissue. Journal of Applied Physiology. 2007; 103:206–219. [PubMed: 17412782]

Hutchinson JR. Shear coefficients for Timoshenko beam theory. Journal of Applied Mechanics. 2001; 68:87–92.

Ishii K, Zhai WG, Akita M, Hirose H. Ultrastructure of the lamina propria of the human vocal fold. Acta Otolaryngologica (Stockholm). 1996; 116:778–782.

Kakita, Y.; Hirano, M.; Ohmaru, K. Physical properties of vocal fold tissue: measurements on excised larynges. In: Stevens, KN.; Hirano, M., editors. Vocal Fold Physiology. University of Tokyo Press; Tokyo: 1981. p. 377-398.

Kelleher JE, Zhang K, Siegmund T, Chan RW. Spatially varying properties of the vocal ligament contribute to its eigenfrequency response. Journal of the Mechanical Behavior of Biomedical Materials. 2010; 3:600–609. [PubMed: 20826366]

Kutty JK, Webb K. Tissue engineering therapies for the vocal fold lamina propria. Tissue Engineering Part B – Reviews. 2009; 15:249–262. [PubMed: 19338432]

Lanir Y, Fung YC. Two-dimensional mechanical properties of rabbit skin – I. Experimental System. Journal of Biomechanics. 1974; 7:29–34. [PubMed: 4820649]

Larsson PO. Determination of Young's and shear moduli from flexural vibrations of beams. Journal of Sound and Vibration. 1991; 146:111–123.

Levenberg K. A method for the solution of certain problems in least squares. Quarterly of Applied Mathematics. 1944; 2:164–168.

Madruga de Melo EC, Lemos M, Aragao Ximenes Filho J, Sennes LU, Nascimento Saldiva PH, Tsuji DH. Distribution of collage in the lamina propria of the human vocal fold. Laryngoscope. 2003; 113:2187–2191. [PubMed: 14660925]

Marquardt D. An algorithm for least squares estimation of nonlinear parameters. SIAM Journal on Applied Mathematics. 1963; 11:431–441.

MATLAB®. The MathWorks. Version 7.10. Natick; Massachusetts, USA:

Min YB, Titze IR, Alipour-Haghighi F. Stress-strain response of the human vocal ligament. Annals of Otology, Rhinology and Laryngology. 1995; 104:563–569.

Ogden RW. Large deformation isotropic elasticity – on the correlation of theory and experiment for incompressible rubberlike solids. Proceedings of the Royal Society of London Series A – Mathematical Physical and Engineering Sciences. 1972; 326:565–584.

Perlman AL, Alipour-Haghighi F. Comparative study of the physiological properties of the vocalis and cricothyroid muscles. Acta Otolaryngologica. 1988; 105:372–378.

Perlman AL, Titze IR. Development of an in vitro technique for measuring elastic properties of vocal fold tissue. Journal of Speech and Hearing Research. 1988; 31:288–298. [PubMed: 3398501]

Perlman AL, Titze IR, Cooper DS. Elasticity of canine vocal fold tissue. Journal of Speech and Hearing Research. 1984; 27:212–219. [PubMed: 6738032]

Qin S, Wang S, Wan M. Improving reliability and accuracy of vibration parameters of vocal folds based on high-speed video and electroglottography. IEEE Transactions on Biomedical Engineering. 2009; 56:1744–1754. [PubMed: 19272979]

Riede T, Lingle S, Hunter EJ, Titze IR. Cervids with different vocal behavior demonstrate different viscoelastic properties of their vocal folds. Journal of Morphology. 2010; 271:1–11. [PubMed: 19603411]

Tao C, Zhang Y, Jiang JJ. Extracting physiologically relevant parameters of vocal folds from high-speed video image series. IEEE Transactions on Biomedical Engineering. 2007; 54:794–801. [PubMed: 17518275]

Titze, IR. Principles of Voice Production. 2nd ed.. National Center for Voice and Speech; Denver: 2000. p. 206

Tran QT, Berke GS, Gerratt BR, Kreiman J. Measurement of Young's modulus in the in vivo human vocal folds. Annals of Otology, Rhinology and Laryngology. 1993; 102:584–591.

Yin FCP, Tompkins WR, Peterson KL, Intaglietta M. A video-dimension analyzer. IEEE Transactions on Biomedical Engineering. 1972; 19:376–381. [PubMed: 5038393]

Zhang K, Siegmund T, Chan RW. A constitutive model of the human vocal fold cover for fundamental frequency regulation. Journal of the Acoustical Society of America. 2006; 119:1050–1062. [PubMed: 16521767]

Zhang K, Siegmund T, Chan RW. A two-layer composite model of the vocal fold lamina propria for fundamental frequency regulation. Journal of the Acoustical Society of America. 2007; 122:1090–1101. [PubMed: 17672656]

Zhang K, Siegmund T, Chan RW. Modeling of the transient responses of the vocal fold lamina propria. Journal of the Mechanical Behavior of Biomedical Materials. 2009; 2:93–104. [PubMed: 19122858]

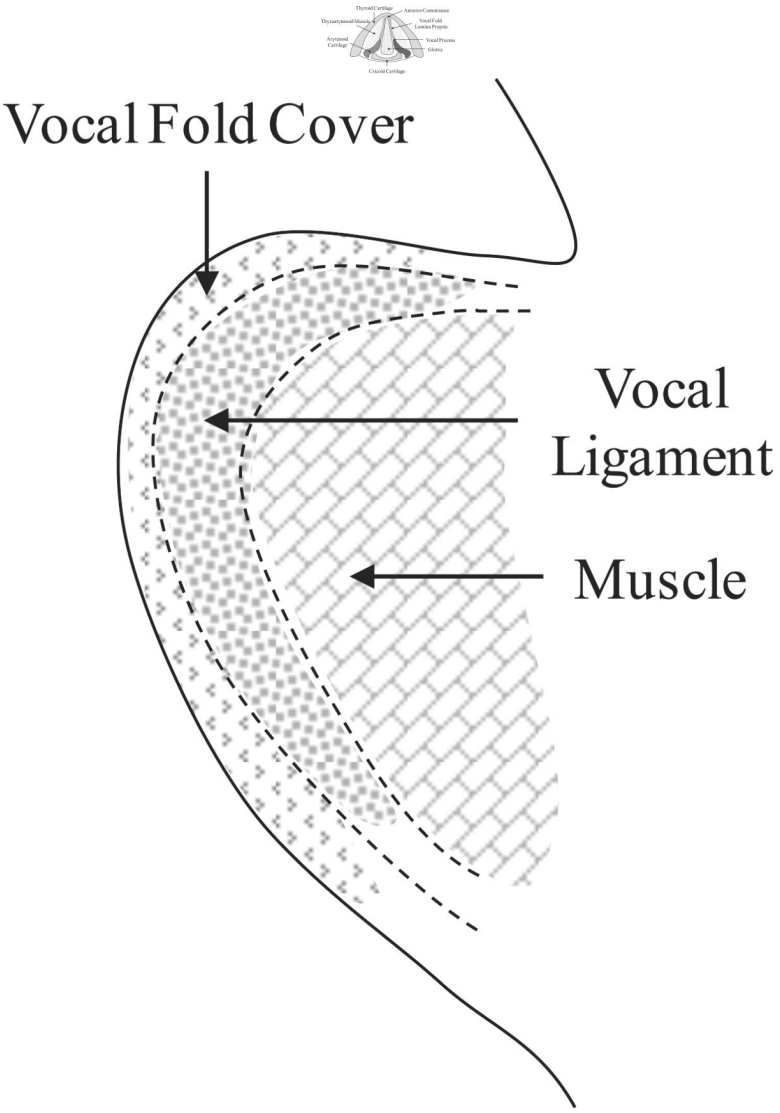

Figure 1.
(a) Schematic superior view of the anatomical structures of the larynx; (b) Coronal cross-section of the vocal fold lamina propria and the thyroarytenoid (vocalis) muscle.

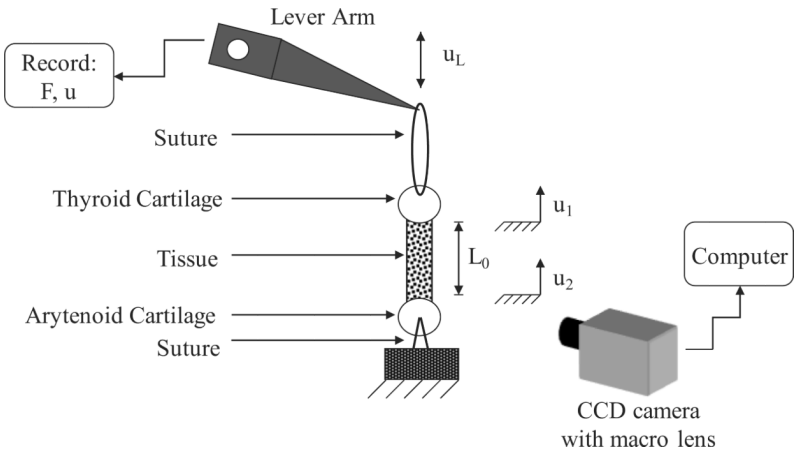

Figure 2.
A schematic of the experimental setup.

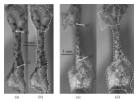

Figure 3.
The undeformed and the deformed images are shown for the 55th load cycle for subject C. The dashed line is the outline of the undeformed specimen (with the cartilage boundaries) superimposed onto the deformed specimen. Images (a) and (b) are the undeformed and deformed states (u_L = 3 mm), respectively, of the vocal ligament specimen. Images (c) and (d) are the undeformed and deformed states (u_L = 4.2 mm), respectively, of the vocal fold cover specimen. Corresponding figures for subjects A and B are provided as online supplemental material.

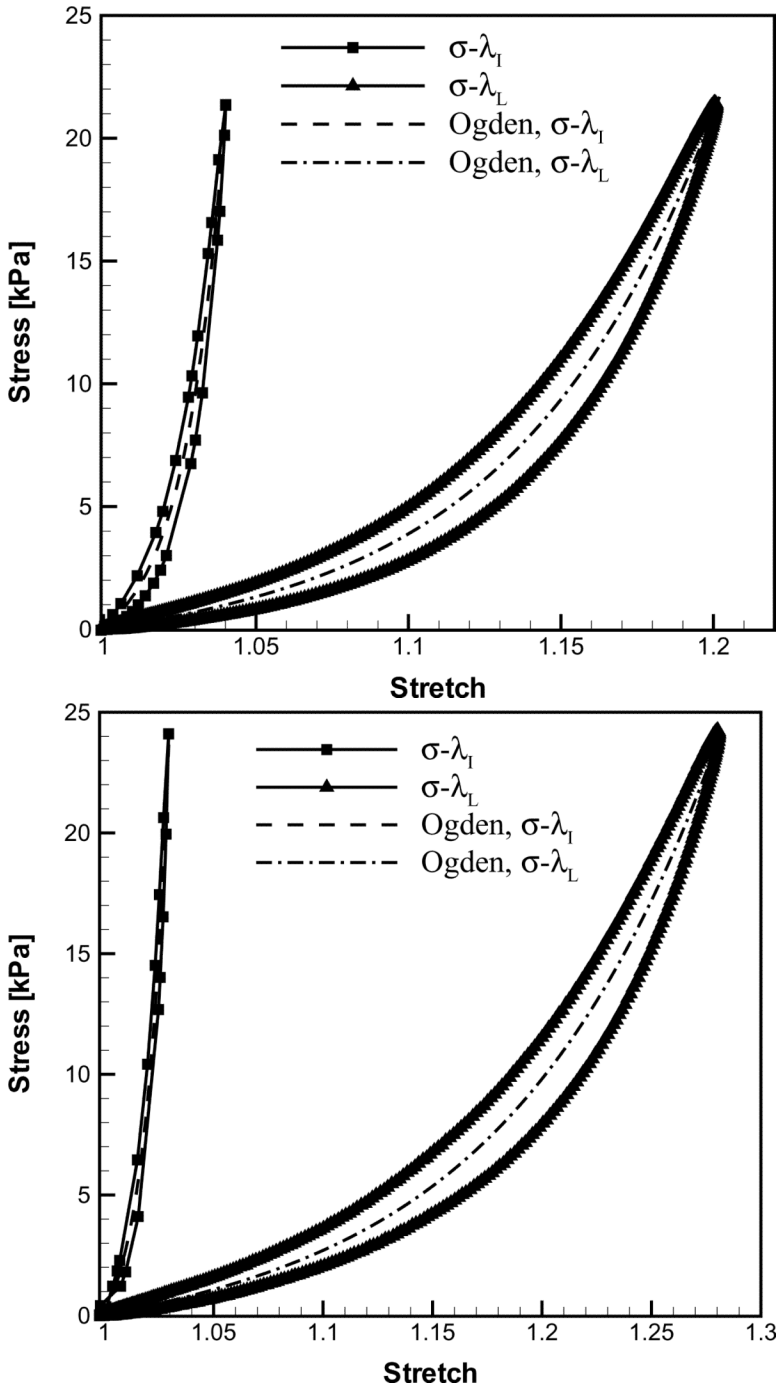

Figure 4.
The stress-stretch curves of the 55th load cycle for subject C: (a) vocal ligament specimen and (b) vocal fold cover specimen.

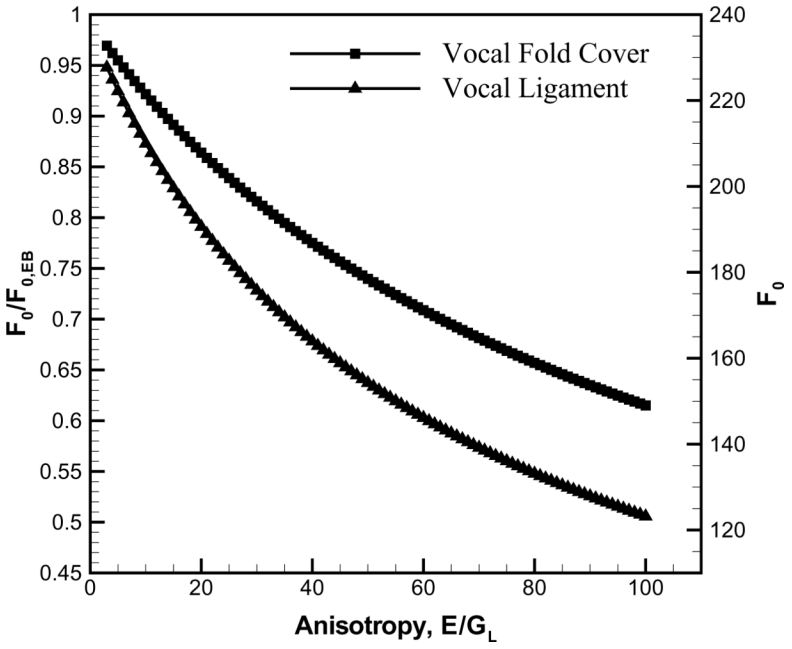

Figure 5.
The effect of transverse shear and rotatory inertia on the fundamental frequency in dependence of tissue anisotropy.

Table 1

Details on the tissue specimens for this study (L_0 = initial vocal fold length; D_0 = initial cross-sectional diameter).

Subject	Gender	Age	Postmortem Hours	Specimen	L_0 [mm]	D_0 [mm]
A	Male	68	20	Ligament	14.3	3.6
				Cover	15.5	2.0
B	Male	68	32	Ligament	21.2	3.4
				Cover	13.8	2.5
C	Male	87	43	Ligament	15.1	3.5
				Cover	15.2	2.9

Table 2

Displacements contributed by the specimen and other sources are tabulated and compared to the applied lever arm displacement, u_L.

Subject	Specimen	u_L [mm]	$u_1 - u_2$ [mm]	$u_{arytenoid}$ [mm]	$u_{thyroid}$ [mm]	U_{other} [mm]
A	Ligament	4.6	0.95	0.77	0.36	2.52
	% of total		21%	17%	8%	55%
	Cover	4.6	1.19	0.87	0.96	1.59
	% of total		26%	19%	21%	34%
B	Ligament	5.0	1.70	0.73	0.68	1.89
	% of total		34%	15%	14%	38%
	Cover	4.4	1.15	0.26	0.47	2.52
	% of total		26%	6%	11%	57%
C	Ligament	3.0	0.58	0.29	0.87	1.27
	% of total		19%	10%	29%	42%
	Cover	4.2	0.46	0.52	0.87	2.35
	% of total		11%	12%	21%	56%

Table 3

Ogden model parameters (with the means and standard deviations, S.D.) based on the images and the lever arm are tabulated with the corresponding R-squared values representing the goodness of fit. C_E and C_α are correction factors defined as $C_E = E_T/E_T$ and $C_\alpha = \alpha_I/\alpha_L$.

		Images			Lever Arm				
Subject	**Specimen**	E_I **[kPa]**	α_I	R^2	E_L **[kPa]**	α_L	R^2	C_E	C_α
A	Ligament	33.0	44.9	0.94	7.4	14.9	0.98	4.5	3.0
	Cover	45.3	43.1	0.99	14.5	18.2	0.99	3.1	2.4
B	Ligament	39.4	40.7	0.98	13.7	18.1	0.99	2.9	2.3
	Cover	20.7	29.3	0.99	13.2	15.5	0.99	1.6	1.9
C	Ligament	110.7	81.6	0.98	20.5	19.7	0.98	5.4	4.1
	Cover	202.1	100.0	0.98	18.6	14.5	0.98	10.9	6.9
Mean S.D.	Ligament	61.0	55.7		13.9	17.6		4.3	3.1
		43.1	22.5		6.6	2.4		1.3	0.9
	Cover	89.4	57.5		15.4	16.1		5.2	3.7
		98.4	37.5		2.8	1.9		4.9	2.7